

# TRPM8 Inhibition Regulates the Proliferation, Migration and ROS Metabolism of Bladder Cancer Cells

This article was published in the following Dove Press journal:  
*OncoTargets and Therapy*

Gang Wang<sup>1-4,\*</sup>  
Rui Cao<sup>5,\*</sup>  
Kaiyu Qian<sup>1-4,\*</sup>  
Tianchen Peng<sup>6</sup>  
Lushun Yuan<sup>6</sup>  
Liang Chen<sup>6</sup>  
Songtao Cheng<sup>6</sup>  
Yaoyi Xiong<sup>6</sup>  
Lingao Ju<sup>1-4</sup>  
Xinghuan Wang<sup>6</sup>  
Yu Xiao<sup>1-4,6</sup>

<sup>1</sup>Department of Biological Repositories, Zhongnan Hospital of Wuhan University, Wuhan, People's Republic of China; <sup>2</sup>Human Genetics Resource Preservation Center of Wuhan University, Wuhan, People's Republic of China; <sup>3</sup>Human Genetics Resource Preservation Center of Hubei Province, Wuhan, People's Republic of China; <sup>4</sup>Cancer Precision Diagnosis and Treatment and Translational Medicine Hubei Engineering Research Center, Wuhan, People's Republic of China; <sup>5</sup>Department of Urology, Beijing Friendship Hospital, Capital Medical University, Beijing, People's Republic of China; <sup>6</sup>Department of Urology, Zhongnan Hospital of Wuhan University, Wuhan, People's Republic of China

\*These authors contributed equally to this work

Correspondence: Yu Xiao; Xinghuan Wang  
Tel +86-27-6781-2689; +86-27-6781-3104  
Fax +86-27-6781-2892  
Email yu.xiao@whu.edu.cn;  
wangxinghuan@whu.edu.cn

**Introduction:** Based on accumulating evidence, transient receptor potential (TRP) ion channels may play important roles in the occurrence and the progression of cancer. TRP melastatin 8 (TRPM8), a member of the TRP family, functions as a Ca<sup>2+</sup>-permeable channel and regulates various physiological and pathological processes. However, the effects of TRPM8 on bladder cancer (BCa) and its underlying mechanisms have not been elucidated.

**Methods:** BCa tissues and matched noncancerous tissues were collected to examine the expression of the TRPM8 mRNA and protein using qRT-PCR, Western blotting and immunofluorescence staining. Meanwhile, the effect of knockdown or inhibition of the activity of the TRPM8 protein on the proliferation, migration and ROS metabolism of bladder cancer cells was detected using the MTT assay, clonogenic survival assay, Transwell chamber migration assay, and reactive oxygen species (ROS) detection, respectively. Furthermore, a mouse model transplanted with BCa cells was established to assess tumor growth after TRPM8 expression was inhibited in vivo.

**Results:** Compared with the noncancerous tissues, the levels of TRPM8 in BCa tissues were significantly increased. Knockdown or inhibition of the activity of the TRPM8 protein in BCa cells reduced cell proliferation and migration. Moreover, the production of ROS was increased in cells treated with siTRPM8, which was accompanied by increased levels of Catalase, HO-1 and SOD2. Furthermore, a mouse model transplanted with the stable TRPM8-deficient T24 cell line was established, demonstrating that knockdown of TRPM8 delayed tumor growth in vivo.

**Discussion:** TRPM8 might play an essential for BCa tumor progression and metastasis by interfering with BCa cell proliferation, motility, ROS metabolism and migration.

**Keywords:** bladder cancer, TRPM8, proliferation, migration, reactive oxygen species

## Introduction

Bladder cancer (BCa) is one of the most common urological malignancies in the world.<sup>1</sup> Although many therapeutic strategies are available for patients with BCa, the recurrence and mortality rates are still high and the mechanism of BCa progression and recurrence remain unclear.<sup>2</sup> Therefore, an urgent need is to identify suitable therapeutic targets and potential molecular pathways underlying BCa progression. Therefore, in previous experiments we collected some human bladder cancer tissues and normal bladder epithelial tissues and performed a microarray analysis.<sup>3</sup> The results of the pathway network analysis revealed that BCa might be associated with the MAPK signaling pathway and calcium signaling pathway.<sup>4</sup>

Meanwhile, several differentially expressed genes involved in the calcium signaling pathway were identified in the mRNA microarray results.<sup>4</sup>

At the cellular level, ion channels and calcium homeostasis are involved in the mechanisms regulating apoptosis, proliferation and differentiation.<sup>5,6</sup> The transient receptor potential (TRP) superfamily of ion channels is divided into families, such as TRPV and TRPM.<sup>7</sup> Most of these proteins are permeable to  $\text{Ca}^{2+}$  or  $\text{Mg}^{2+}$  and are involved in various physiological and pathological processes.<sup>8</sup> In addition, over the past few decades, transient receptor potential ion channels have consistently been shown to be related to tumorigenesis and development in various cancers.<sup>5</sup> A histone deacetylase inhibitor (HDACi) inhibits the growth of BCa T24 cells by enriching H3K9Ac at the TRPM2 promoter and upregulating its expression.<sup>9</sup> As shown in our previous study, TRPM7, a  $\text{Mg}^{2+}/\text{Ca}^{2+}$ -permeable channel, is essential for BCa cell proliferation, motility and apoptosis and closely interacts with the MAPK signaling pathway.<sup>4</sup>

TRPM8, another member of the TRPM superfamily, is associated with the Gleason score and the TNM stage and is reported as a biomarker for prostate cancer.<sup>10</sup> According to the results of in vitro and in vivo experiments, TRPM8 alters the proliferation and efficacy of epirubicin chemotherapy in prostate cancer.<sup>11–14</sup> Meanwhile, TRPM8 was recently reported to be abnormally expressed in other cancers, including breast cancer, pancreatic adenocarcinoma, osteosarcoma, and BCa.<sup>15–17</sup> Ceylan et al observed a significant decrease in the expression of TRPM8 in bladder cancer tissues using qRT-PCR and immunohistochemistry analysis.<sup>18</sup> In contrast, Xiao et al reported a significant upregulation of TRPM8 in BCa tissues compared with matched noncancerous tissues, and its expression was associated with the histological grade and tumor stage.<sup>19</sup> Based on these controversial results, the association between the expression of TRPM8 and the development of BCa must be clarified. Menthol, an important component of peppermint oil, increases the intracellular calcium concentration via the TRPM8 channel. After menthol treatment, the viability of T24 cells is reduced in a dose-dependent manner.<sup>20</sup> Therefore, we hypothesized that TRPM8 would affect the biological behaviors of bladder cancer cells, but its effects on pathogenesis of BCa have not yet been clarified.

Overall, the purpose of this study is to investigate the correlation between bladder cancer and TRPM8 expression levels, and to elucidate the potential mechanism

underlying the effects of TRPM8 gene silencing or its antagonists.

## Materials and Methods

### Human Bladder Tissue Samples

As described in the study by Cao et al from our group,<sup>4</sup> the stage II bladder cancer tissue samples ( $n = 17$ ) and matched paracancerous tissues samples ( $n = 17$ ) were obtained from male patients (ages  $62.88 \pm 5.34$ ) after radical cystectomy, and three normal bladder tissue samples were obtained after an accidental death from donors at Zhongnan Hospital of Wuhan University. Informed consent was obtained from all subjects to collect the samples, and it was conducted in accordance with the Declaration of Helsinki. Histological diagnosis of the bladder tissues were by two pathologists. The tissue samples were fixed with 4% paraformaldehyde (PFA) for subsequent immunofluorescence staining or snap frozen and stored in liquid nitrogen for subsequent RNA isolation. This study was approved by the Ethics Committee of Zhongnan Hospital of Wuhan University (approval number: 2015029) ([Supplementary Materials 1](#)). The sample collection and treatment procedures were conducted in accordance with the approved guidelines.

### BCa Cell Lines

The T24 human BCa cell line (transitional cell carcinoma, Cat. #SCSP-536) was acquired from the Chinese Academy of Sciences in Shanghai, China. The EJ human BCa cell line (carcinoma, Cat. #CL-0274) was purchased from Procell Co. Ltd., Wuhan, China. The cells were identified by the China Center for Type Culture Collection in Wuhan, China. T24 and EJ cells were cultured in RPMI-1640 medium (containing 1% penicillin G sodium/streptomycin sulphate and 10% fetal bovine serum) in an atmosphere containing 5%  $\text{CO}_2$  at 37 °C.

### RNA Extraction, Reverse Transcription and Quantitative Real-Time PCR (qRT-PCR)

Total RNA was isolated from BCa cells and tissues using the RNeasy Mini Kit from Qiagen (Cat. #74101) and QIAshredder (Qiagen, Cat. #79654), according to the manufacturer's protocol. The concentration of total RNA was measured with a NanoPhotometer (Implen, Cat. #N60). The ReverTra Ace qPCR RT Kit (Toyobo, Cat. #FSQ-101) was used for the reverse transcription. 500 ng

cDNA templates were added to a PCR system with a final volume of 25  $\mu$ L. All primers used in our study were tested for optimal annealing temperatures and PCR conditions were optimized with gradient PCRs on a Bio-Rad iCycler (Cat. #CFX96). Primer sequences are listed in [Supplementary Table S1](#). The mRNA expression levels of each gene were normalized to GAPDH.

## Knockdown of TRPM8 in BCa Cells

TRPM8-target specific siRNA and lentiviral small hairpin RNA (LV-shRNA) were purchased from Genescript Ltd. in Suzhou, China. The T24 and EJ BCa cells were transfected with the TRPM8-target specific siRNA (siTRPM8) using Lipofectamine 2000 (Invitrogen, Cat. #11668-027), according to the manufacturer's protocol. The sense sequence of the siRNAs were as follows: siTRPM8-1 (5'-GGAGTC TGCTGACCTTCAA -3'), siTRPM8-2 (5'-GCTGTGGC TTTGTATCATT-3'), siTRPM8-3 (5'-GGATATTC CGTT CGGTCAT-3'), and si-control (5'-UUCUCCGAACGU GUCACGUTT-3'). The qRT-PCR, Western blotting and immunofluorescence staining analyses were performed to evaluate alterations in the levels of the TRPM8 mRNA and protein at 48 h after the siTRPM8 transfection. T24 BCa cells were infected with lentiviral-TRPM8-shRNA (LV-M8sh) and lentiviral-control-shRNA (LV-NC), and then treated with 0.8 mg/mL puromycin for approximately 14 days to select antibiotic-resistant, stably transfected cells.

## MTT Assay

Forty-eight hours after transfection, cells were seeded in 96-well plates (2,000 cells per 200  $\mu$ L of medium) and cultured for 48 h before 10  $\mu$ L of 5 mg/mL MTT were added to each well and incubated for 4 h at room temperature. The medium was removed from the 96-well plate and 100  $\mu$ L of DMSO were added to dissolve the formazan precipitate. A microplate reader was used to measure the absorbance at 490 nm and assess cell viability (Molecular Devices, Cat. # SpectraMax M2).

## Clonogenic Survival Assay

Forty-eight hours after transfection, BCa cells were seeded in 6-well plates (800 cells per well) and cultured for 2 weeks. When colonies were visible, the cells were fixed with 4% paraformaldehyde for 30 min and then stained with 0.1% crystal violet. The numbers of colonies were counted with the naked eyes and a phase contrast microscope.

## ROS Detection by Staining Cells with DCFH-DA

Intracellular ROS levels were evaluated using the fluorescent probe 2',7'-dichlorofluorescein diacetate (DCFH-DA). Cells were transfected and cultured for 48 hours. Cells were collected, washed, and resuspended in 1 mL serum-free medium containing 10  $\mu$ M DCFH-DA (Sigma-Aldrich, Cat. # D6883) at 37°C for 30 min. Thereafter, the cells were washed three times with serum-free medium and subjected to a flow cytometry analysis. For DCFH-DA fluorescence staining, transfected BCa cells cultured on glass slides were stained with DCFH-DA for 30 min at room temperature and then washed three times with PBS. Nuclei were counterstained with DAPI for 10 min at room temperature. Images of the fluorescent dye were captured with a fluorescence microscope (Olympus, Cat. #IX73).

## Transwell Chamber Migration Assay

For the migration assay, 200  $\mu$ L serum-free medium containing  $6 \times 10^4$  cells were seeded in the upper transwell chambers (Corning, Cat. #3450). Medium containing 10% FBS was added to the lower chambers to induce cell migration. After culture for 24 h, the cells were fixed with 4% paraformaldehyde, washed with PBS and stained with 0.1% crystal violet. The numbers of migrated cells were counted using a phase contrast microscope and statistically analyzed.

## (4-Tertbutylphenyl)-4-(3-Chloropyridin-2-Yl)Tetrahydropyrazine-1(2H)-Carbox-Amide (BCTC) Treatment of BCa Cells

BCa T24 cells were seeded in 6-well plates, cultured for 24 h, and then treated with 0, 20 or 40  $\mu$ M BCTC (Sigma-Aldrich, Cat. #SML0355) for 48 h. Alterations in proliferation and migration were measured using the MTT assay, Ki-67 immunofluorescence staining and transwell chamber migration assay, respectively.

## Western Blot Analysis

For this assay, 7.5–12.5% SDS-PAGE gels were used to separate total protein isolated from cells, and the proteins were subsequently transferred to PVDF membrane (Millipore, Cat. #IPVH00010). Membranes were blocked with 5% fat-free milk for 2 h at room temperature and incubated with primary antibodies ([Supplementary Table S2](#)) for 12 h at 4°C. After being washed three times with T-BST, membranes were incubated with an HRP-conjugated

secondary antibody ([Supplementary Table S3](#)) for 2 h. Bands were detected using an enhanced chemiluminescence kit (Bio-Rad, Cat. #1705060) and exposed to Kodak Biomax MR Films.

## Immunofluorescence Staining

All tissues samples were fixed with 4% paraformaldehyde overnight at 4 °C and then embedded in paraffin using a tissue processor (Thermo Fisher Scientific, Cat. #STP 120). Paraffin sections (5 µm) were cut with a rotation microtome (Thermo Fisher Scientific, Cat. #HM325). Sections were blocked with 10% goat serum at room temperature for 45 min, and then serially incubated with the indicated primary antibody ([Supplementary Table S2](#)) and Cy3-labeled or FITC-labeled secondary antibody ([Supplementary Table S3](#)) in a humidified atmosphere. Nuclei were counterstained with DAPI for 10 min at room temperature. Images of fluorescently labeled tissue sections were captured with a fluorescence microscope (Olympus, Cat. #IX73).

## Hematoxylin and Eosin (H&E) Staining

All sections were deparaffinized and rehydrated in xylene, 100%, 96%, 80%, 70% ethanol and H<sub>2</sub>O, and then stained with 10% hematoxylin (Sigma-Aldrich) for 7 min. After washes with water for 10 min, 1% eosin in 0.2% glacial acetic acid was used to stain the cytoplasm. The sections were washed with water and dehydrated in 70%, 80%, 96%, and 100% ethanol and xylene. Images were captured using an inverted phase contrast microscope (Leica, Cat. #DMI 1).

## Xenograft Model

Ten 3-week-old male NOD/SCID mice were purchased from Beijing Vital River Laboratory Animal Technology Co., Ltd. (Beijing, China). The mice were housed in an SPF environment in the laboratory animal facility of Zhongnan Hospital of Wuhan University for one week. Ten male NOD/SCID mice were subcutaneously injected with T24 cells infected with lentiviral-TRPM8-shRNA (n = 5) and lentiviral-control-shRNA (n = 5) in the dorsal area near the forelimbs. Cells were resuspended in 100 µL of PBS at a concentration of  $2 \times 10^7$  cells/mL. Calipers were used to measure the dimensions of the tumor, and the tumor size was calculated with the following formula: Tumor size = length  $\times$  width<sup>2</sup>  $\times$  0.5 mm<sup>3</sup>. After observing tumor growth for 46 days, the mice were sacrificed by cervical dislocation to collect

tumor tissues. The animal experiment was in accordance with animal welfare and European animal care guidelines,<sup>21</sup> and approved by the Institutional Animal Care and Use Committee at Center for Animal Experiment, Wuhan University (approval number: 2018152) ([Supplementary Materials 2](#)).

## Statistical Analyses

All experiments were repeated at least three times. Statistical analyses were performed using SPSS 16.0 software. Two-tailed Student's t-tests were used to evaluate the statistical significance of differences in data. P-values <0.05 were considered to be significant.

## Results

### TRPM8 Expression Was Upregulated in BCa Tissues

Double immunofluorescence staining was performed to investigate TRPM8 expression in BCa tissues (n = 3), matched paracancerous tissues (n = 3) and normal bladder tissues (n = 3). OCT-4 was used as a marker of BCa cells. More TRPM8 and OCT-4 double-labeled cells were detected in the BCa tissues than the matched paracancerous bladder tissues and normal bladder tissues ([Figure 1A](#)), consistent with a previous study.<sup>19</sup> Meanwhile, we performed qRT-PCR analysis to evaluate the mRNA expression levels of TRPM8. Compared with the matched paracancerous tissues (n = 17), TRPM8 was significantly upregulated in the BCa tissues (n = 17) ([Figure 1B](#)). In addition, the bladder cancer data collected from the TCGA database revealed increased levels of the TRPM8 mRNA in BCa (P<0.05) ([Figure 1C](#)).

### Downregulation of TRPM8 Reduced the Viability and Proliferation of BCa Cells

We constructed a TRPM8 knockdown cell model by transfecting an siRNA into BCa cell lines to investigate the function of TRPM8 in bladder cancer. We treated the BCa cells with three TRPM8 target-specific siRNAs, and then validated the knockdown efficiencies using qRT-PCR ([Figure 1D](#)) and Western blotting ([Figure 1E](#)) at 48 h after transfection. Moreover, immunofluorescence staining revealed a substantial decrease in the level of the TRPM8 protein in cells transfected with the siRNAs ([Supplementary Figure S1](#)). Based on these results, TRPM8 expression was decreased at both the mRNA



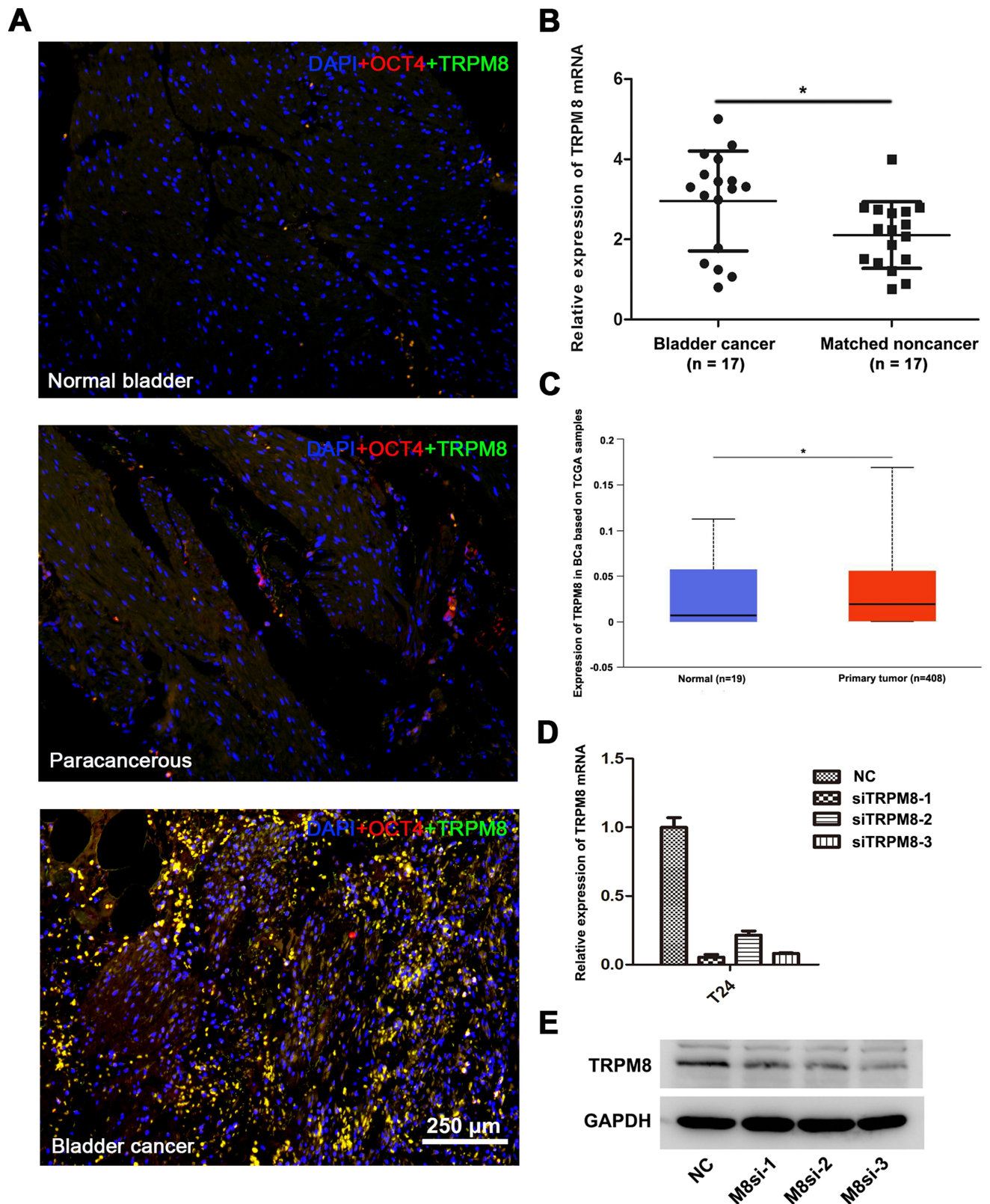


**Figure 1** TRPM8 expression in BCa tissues. **(A)** Immunofluorescence staining for TRPM8 (green) in normal bladder tissues, paracancerous tissues and BCa tissues. OCT-4 (red) was used as a marker of BCa cells, and nuclei were stained by DAPI (blue). The scale bar represents 250  $\mu$ m. **(B)** qRT-PCR analysis of the expression of TRPM8 mRNA in BCa (n = 17) and matched paracancerous tissues (n = 17). **(C)** Increased expression of TRPM8 in BCa tissues from the TCGA database was analyzed. **(D)** qRT-PCR validated the efficacy of knockdown at mRNA level by TRPM8 target-specific siRNA (siTRPM8) in BCa T24 cells. **(E)** Western blot analysis validated the efficacy of knockdown at the protein level by the TRPM8 target-specific siRNA (siTRPM8) in T24 BCa cells. \* $p$ <0.05.

and protein levels in the knockdown cell model. Thus, siTRPM8-3 was used in the subsequent experiments.

T24 and EJ cells were transfected with TRPM8 target-specific siRNA (siTRPM8 group) and negative control siRNA (NC group) for 48 h and analyzed using the MTT assay to determine the effect of TRPM8 on the viability and proliferation of BCa cells, suggesting that TRPM8 knockdown inhibited BCa cell proliferation ([Figure 2A](#) and [Supplementary Figure S2](#)). Moreover, the clonogenic survival assay revealed a significant decrease in the number of colonies formed by TRPM8 siRNA-treated T24 ([Figure 2B](#) and [C](#)) and EJ BCa cells ([Supplementary Figure S3A](#) and [B](#)) compared with the NC group.

### Induction of ROS Accumulation in TRPM8-Deficient BCa Cells

The ROS levels in T24 BCa cells transfected with either the NC or TRPM8 siRNA for 48 h were detected using flow cytometry. The siTRPM8 group exhibited greater ROS accumulation than the NC group ([Figure 2E](#) and [F](#)). Consistently, an increased percentage of ROS-positive cells was observed in the siTRPM8 group after DCFH-DA staining using a fluorescence microscope ([Figure 2D](#)). Western blot analysis revealed increased levels of proteins associated with ROS metabolism (Catalase, HO-1 and SOD2) and decreased levels of SIRT1 in the BCa cells that had been transfected with the TRPM8 siRNA for 48h ([Figure 2I](#)).

### TRPM8 Knockdown Suppressed BCa Cell Migration

Transwell migration assay was used to measure cell migration. Migration rates were significantly decreased in the TRPM8 siRNA-treated BCa cells T24 ([Figure 2G](#) and [H](#)) and EJ ([Supplementary Figure S4A](#) and [B](#)).

Proteins involved in tumor metastasis, including  $\beta$ -catenin, vimentin, paxillin and snail, were analysed using Western blotting ([Figure 2I](#)). The results revealed decreased levels of  $\beta$ -catenin, vimentin, paxillin and snail in siTRPM8 group. Meanwhile, the activation of ERK1/2 and p38, two members of the MAPK signaling pathway, was altered in the T24 cells transfected with the TRPM8 siRNA. The levels of phosphorylated ERK1/2 (p-ERK1/2) and phosphorylated p38 (p-p38) were reduced in the siTRPM8 group. In addition, Western blotting results also revealed changes in the AKT/GSK3 $\beta$  signaling pathway, as p-AKT levels were

decreased and p-GSK3 $\beta$  levels were increased in TRPM8-deficient cells ([Figure 2I](#)).

### BCTC, an Antagonist of TRPM8, Inhibited BCa Cell Proliferation and Migration

T24 cells were treated with different concentrations (0, 2.5, 5, 10, 20, 40, 60 or 80  $\mu$ M) of BCTC for 48 h and proliferation was measured using the MTT assay to optimize the effect of BCTC on cell viability. Compared to the 0  $\mu$ M group, the viability of T24 cells was considerably inhibited by the BCTC treatment for 48 h in a dose-dependent manner ([Figure 3B](#)). The proliferation of T24 cells treated with 0, 20 and 40  $\mu$ M BCTC for 48 h was detected using Ki-67 immunofluorescence staining. Ki-67 is an important marker of proliferating cells. Compared to the 0  $\mu$ M group, the number of Ki-67 positive BCa cells (green) was substantially reduced by treatments with 20 and 40  $\mu$ M BCTC for 48 h ([Figure 3A](#)). Meanwhile, cell migration was measured using transwell migration assay. After 48 h of treatment with BCTC, the relative migration rate of T24 cells was significantly decreased compared to the control groups ([Figure 3C](#) and [D](#)).

### Effect of TRPM8 on BCa Cell Growth in vivo

T24 cells were infected with lentiviral-TRPM8-shRNA (LV-M8sh) or lentiviral-control- shRNA (LV-NC) to establish a stable TRPM8-deficiency T24 cells line or the control T24 cells line, respectively, and to examine the effect of TRPM8 knockdown on BCa cell growth in vivo. The knockdown efficiency of the shRNA was validated by performing qRT-PCR ([Figure 4A](#)) and immunofluorescence staining ([Figure 4B](#)), indicating that TRPM8 was remarkably silenced at both the mRNA and protein levels in the T24 cells infected with LV-M8sh. Then, the T24 LV-M8sh cells or T24 LV-NC cells were subcutaneously injected into the dorsal area of the NOD/SCID mice near the forelimbs. The tumor size was measured with a caliper approximately two weeks after the cells were injected. As shown in [Figure 4D](#), compared with the T24 LV-NC group, tumor growth was significantly inhibited in the T24 LV-M8sh group. After the specified observation period, tumor-bearing mice were sacrificed by cervical dislocation, and the tumors were dissected from subcutis of tumor-bearing mice ([Figure 4C](#)). The dissected tumors were embedded in paraffin and stained with H&E. The number of tumor cells was decreased in the LV-M8sh

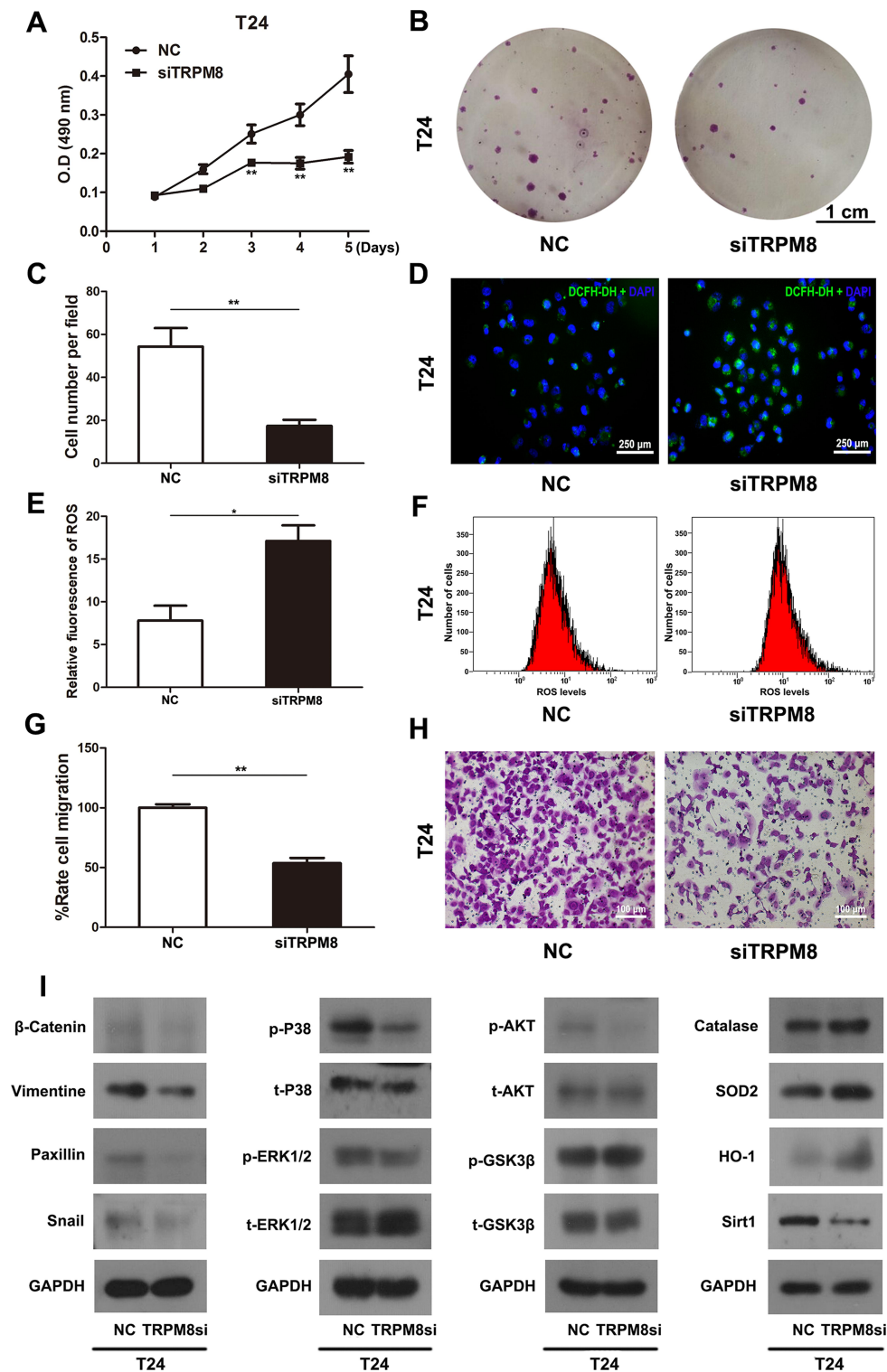


**Figure 2** Effect of TRPM8 on BCa T24 cells. **(A)** The cell viability was analyzed by MTT assay using T24 cells treated by TRPM8 target-specific-siRNA (siTRPM8) and negative-control-siRNA (NC). **(B)** Clonogenic survival assay was performed to measure the proliferation of T24 cells after siRNA transfection for 48 h and culture in 6-well plates for 15 days. The scale bar represents 1 cm. **(C)** The cell number per field in the clonogenic survival assay was counted and statistically analyzed. **(D)** Representative images of DCFH-DA staining of ROS (green) in T24 cells transfection with siRNA. Nuclei were stained with DAPI (blue). The scale bar represents 250  $\mu$ m. **(E)** Statistical analysis of the relative fluorescence of ROS in T24 cells after the siRNA transfection. **(F)** The ROS level was detected in T24 cells after siRNA transfection using flow cytometry. **(G)** Statistical analysis of the results of the transwell migration assay. **(H)** Transwell migration assay was performed to measure the migration of T24 cells after siRNA transfection. The scale bar represents 100  $\mu$ m. **(I)** Western blot analyses of the levels of proteins involved in cell viability, ROS metabolism and migration. GAPDH served as a loading control. All values are presented the mean  $\pm$  SD of triplicate measurements, and the experiments were repeated three times with similar results, \* $p < 0.05$ , \*\* $p < 0.01$ .



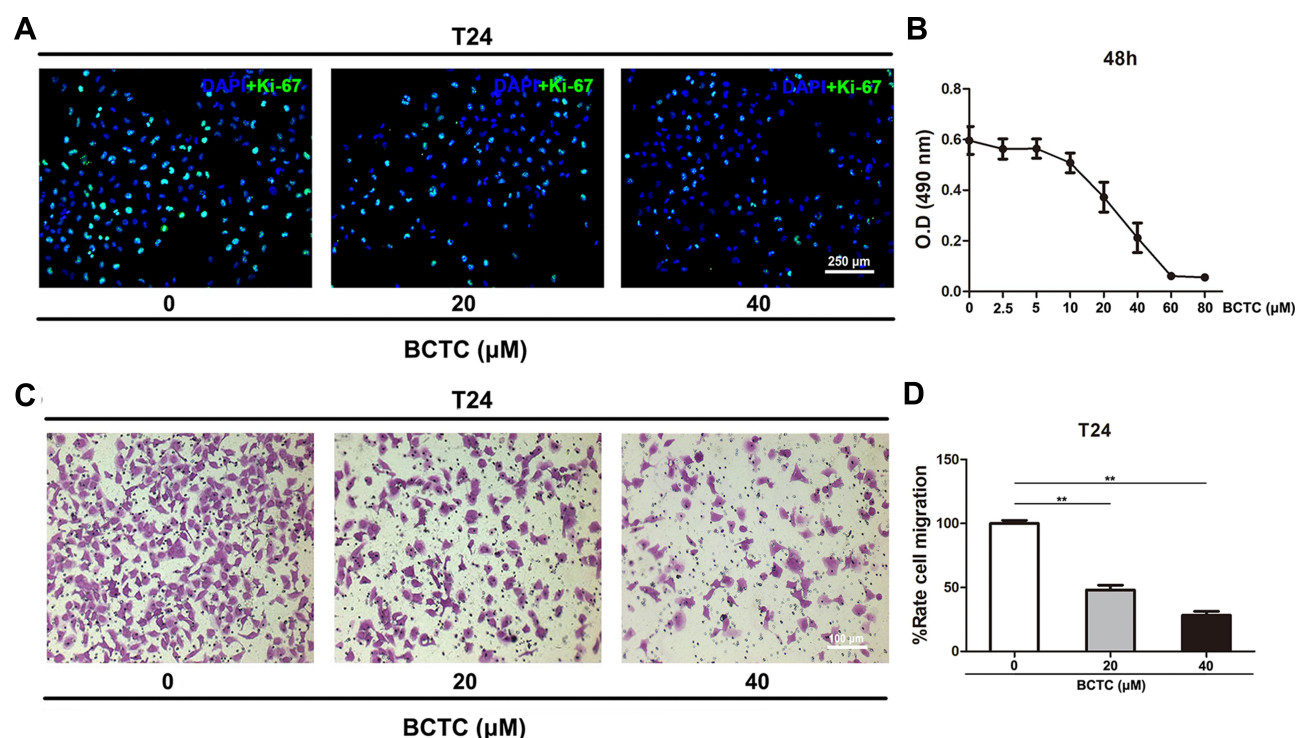


**Figure 3** BCTC reduces the viability and migration of T24 cells. **(A)** Immunofluorescence staining of Ki-67 (green) in T24 cells treated with 0, 20 or 40  $\mu$ M BCTC for 48 h. Nuclei were stained by DAPI (blue). The scale bar represents 250  $\mu$ m. **(B)** The viability of T24 cells treated with different concentrations of BCTC (0, 2.5, 5, 10, 20, 40, 60 or 80  $\mu$ M) for 48 h was evaluated using the MTT assay. **(C)** Transwell migration assay was performed to measure the migration of T24 cells that had been pretreated with 0, 20 or 40  $\mu$ M BCTC for 48 h. The scale bar represents 100  $\mu$ m. **(D)** The relative cell migration rate was calculated and a statistical analysis was performed. All values are presented as the mean  $\pm$  SD of triplicate measurements and the experiments were repeated three times with similar results, \*\* $p < 0.01$ .

group compared with the LV-NC group (Figure 4E). Immunofluorescence staining analysis revealed intensities of TRPM8 staining in tumors from the LV-M8sh group, which indicated a persistently reduced level of TRPM8 over an extended period. Moreover, fewer Ki-67 positive cells were detected and the intensity of SOD2 staining was increased in tumors from the LV-M8sh group compared with the control group (Figure 4F), consistent with the results of the in vitro experiments (Figure 2I).

## Discussion

Bladder cancer is one of the most common urinary tract tumors. The current gold standard for diagnosis is cystoscopy biopsy. However, if the tumor is small, its biopsy will mainly depend on the experience and skills of the clinician. Therefore, the identification of new biomarkers for the diagnosis and treatments of bladder cancer is important. We performed a transcriptome analysis of bladder cancer tissues and normal bladder tissues, and the results suggested that the calcium signaling pathway and MAPK signaling pathway were significantly associated with BCa. TRPM8, a  $\text{Ca}^{2+}$ -permeable channel, is an important member of the TRPM

family. After T24 BCa cells were treated with a TRPM8 agonist, the intracellular calcium concentration was increased and cell viability was reduced, indicating that TRPM8 was essential for bladder cancer cell viability.<sup>20</sup> However, differences in TRPM8 expression in bladder cancer tissues have been reported. Immunofluorescence staining and qRT-PCR were used to assess TRPM8 expression, and its expression was significantly upregulated at both transcriptional and protein levels in the BCa tissues compared with the matched paracancerous tissues, consistent with the findings reported by Xiao et al.<sup>19</sup>

We transfected the BCa cell lines with the TRPM8 target-specific siRNA to analyze the function of TRPM8 in bladder cancer, and observed that TRPM8 knockdown inhibited the proliferation and colony formation ability of BCa cells. In addition, in the TRPM8-deficient cell model, the ROS level and number of ROS-positive cells were significantly increased. A modest increase in the ROS level in cancer cells is essential for tumor progression, whereas an excess level might suppress tumors growth.<sup>22</sup> Catalase, HO-1 and SOD2 are important proteins involved in ROS metabolism. Catalase protects chromosomes from damage induced by



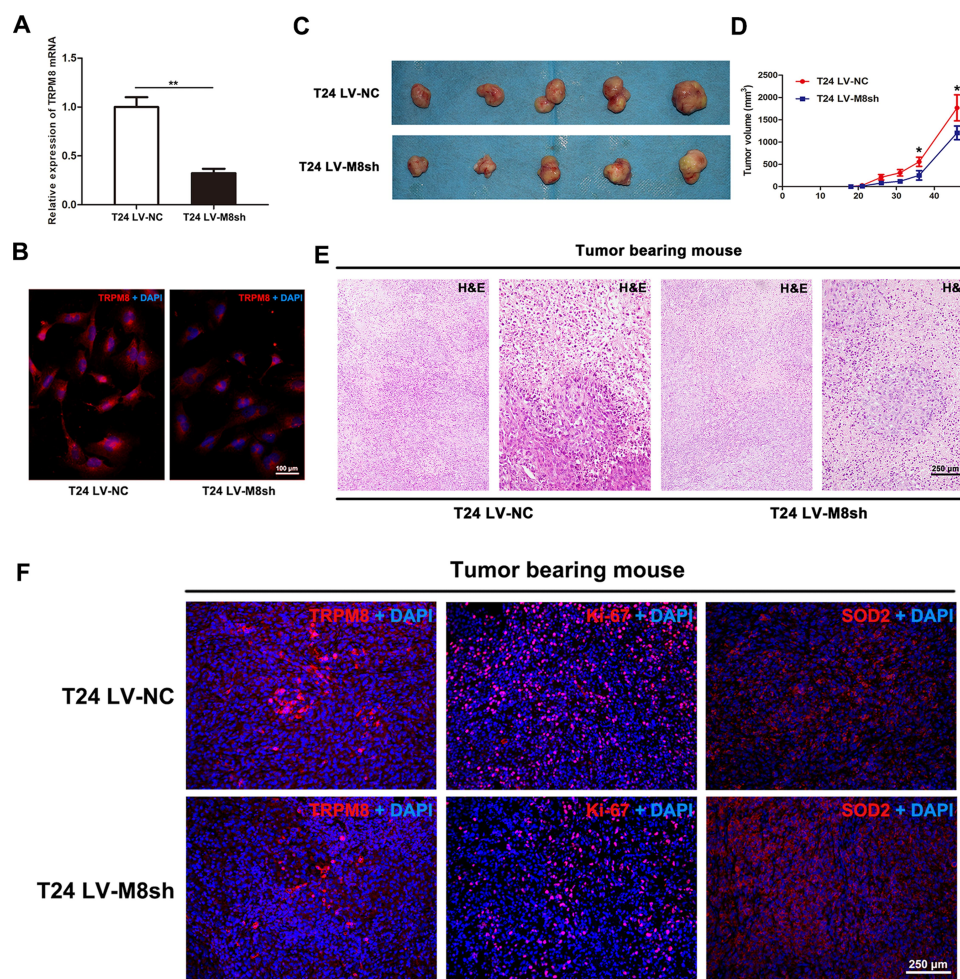


**Figure 4** Downregulation of TRPM8 inhibits bladder cancer growth in vivo. **(A)** qRT-PCR validated the efficacy of TRPM8 knockdown at the mRNA level by LV-M8sh and LV-NC in BCa T24 cells. **(B)** Immunofluorescence staining validated the efficacy of TRPM8 knockdown at the protein level by LV-M8sh and LV-NC in BCa T24 cells. **(C)** NOD/SCID mice were subcutaneously injected with T24 LV-M8sh or T24 LV-NC cells and allowed to grow for 46 days. **(D)** Statistical analysis of the sizes of tumors excised from tumor-bearing NOD/SCID mice. The tumor volume was measured 6 times, \* $p < 0.05$ . **(E)** Representative images of hematoxylin and eosin (H&E) staining in tumor tissues dissected from tumor-bearing NOD/SCID mice. The scale bar represents 250  $\mu$ m. **(F)** Immunofluorescence staining for TRPM8, Ki-67 and SOD2 in tumor tissues dissected from tumor-bearing NOD/SCID mice. Nuclei were stained with DAPI (blue). The scale bars represent 250  $\mu$ m.

oxidative stress or ionizing radiation, and thus plays a role in inhibiting cell death.<sup>23</sup> HO-1 is a redox-sensitive enzyme with antioxidant and antiapoptotic effects.<sup>24</sup> SOD2 sufficiently reduces mitochondrial ROS production and protects against cell death.<sup>25</sup> Moreover, SIRT1 is also associated with ROS accumulation.<sup>26,27</sup> As shown in our previous study, the activation of the PPAR $\gamma$ -SIRT1 feedback loop promotes ROS production and increases the expression of SOD2 and Catalase. Excess ROS were produced, resulting in the oxidative stress and subsequent death of bladder cancer cells.<sup>26,27</sup> In the present study, Catalase and SOD2 levels were increased in the siTRPM8 group and SIRT1 expression was downregulated, subsequently inducing ROS accumulation. However, further studies are needed to clarify the underlying mechanism by which TRPM8, the PPAR $\gamma$ -SIRT1 feedback loop, and ROS metabolism contribute to tumorigenesis in bladder cancer.

Cancer cell migration and invasion are the most critical steps in cancer progression. Therefore, we performed transwell migration assay to measure the cell migration. Compared with the NC group, the migration rates were significantly decreased in the siTRPM8 group. Meanwhile, the levels of proteins involved in the epithelial-mesenchymal transition (EMT) ( $\beta$ -catenin, vimentin, paxillin and snail) were decreased. The EMT is a process by which epithelial cancer cells gradually lose their characteristics and acquire the phenotype of mesenchymal cells,<sup>28</sup> which is directly and indirectly regulated by multiple molecular mechanisms, including the MAPK and PI3K signaling pathways.<sup>29,30</sup> The activation of ERK1/2 and p38, key members of the MAPK family, were altered in the TRPM8 target-specific-siRNA treated T24 cells. In the siTRPM8

group, the levels of phosphorylated ERK1/2 (p-ERK1/2) and phosphorylated p38 (p-p38) were decrease, comparing to the NC group. In addition, we also observed changes in the AKT/GSK3 $\beta$  signaling pathway in the TRPM8-deficient cells.

BCTC, a potent antagonist of TRPM8, inhibits TRPM8 activity without reducing its expression.<sup>31</sup> After treatment with different concentrations of BCTC, the proliferation ability of T24 cells was inhibited in a dose-dependent manner. Ki-67 is a proliferation-associated nuclear antigen.<sup>32</sup> We performed Ki-67 immunofluorescence staining to detect cell proliferation of T24 cells after treatment with BCTC. Compared to the control group, the number of Ki-67 positive BCa cells (green) was significantly decreased in the BCTC treatment group. In addition, the migration rate of the BCTC treated T24 cells was decreased.

TRPM8 altered the proliferation, ROS metabolism and migration of bladder cancer cells in vitro. Subsequently, we established a NOD/SCID mouse model transplanted with lentiviral-shRNA treated T24 cells and observed a significant delay in tumor growth following the silencing of TRPM8. Compared with the control group, a substantial increase in SOD2 levels was observed in the tissues from the lentiviral-shRNA-treated tumor-bearing mice using immunofluorescence staining. Overall, further studies are needed to elucidate the underlying mechanisms and deep insights into the effect of TRPM8 in BCa.

## Conclusion

The results of the in vitro and in vivo experiments performed in the present study have demonstrated that the silencing of TRPM8 or inhibition of the TRPM8 protein reduce the proliferation and migration rates of BCa cells and induce ROS accumulation and deactivation of the MAPK and AKT/GSK3 $\beta$  signaling pathways in bladder cancer cells.

## Funding

This study was supported in part by grants from the National Natural Science Foundation of China (grant number 81902603), the Health commission of Hubei Province scientific research project (grant number WJ2019H013) and the Fundamental Research Funds for the Central Universities (grant number 2042019kf0176).

## Disclosure

The authors report no conflicts of interest in this work.

## References

1. Antoni S, Ferlay J, Soerjomataram I, Znaor A, Jemal A, Bray F. Bladder cancer incidence and mortality: a global overview and recent trends. *Eur Urol*. 2017;71(1):96–108. doi:10.1016/j.eururo.2016.06.010
2. Flaig TW, Spiess PE, Agarwal N, et al. NCCN guidelines insights: bladder cancer, version 5.2018. *J Natl Compr Canc Netw*. 2018;16(9):1041–1053. doi:10.6004/jncn.2018.0072
3. Wang G, Cao R, Wang Y, et al. Simvastatin induces cell cycle arrest and inhibits proliferation of bladder cancer cells via PPAR $\gamma$  signalling pathway. *Sci Rep*. 2016;6:35783. doi:10.1038/srep35783
4. Cao R, Meng Z, Liu T, et al. Decreased TRPM7 inhibits activities and induces apoptosis of bladder cancer cells via ERK1/2 pathway. *Oncotarget*. 2016;7(45):72941–72960. doi:10.18632/oncotarget.12146
5. Shapovalov G, Ritaine A, Skryma R, Prevarskaya N. Role of TRP ion channels in cancer and tumorigenesis. *Semin Immunopathol*. 2016;38(3):357–369. doi:10.1007/s00281-015-0525-1
6. Danese A, Patergnani S, Bonora M, et al. Calcium regulates cell death in cancer: roles of the mitochondria and mitochondria-associated membranes (MAMs). *Biochim Biophys Acta*. 2017;1858(8):615–627. doi:10.1016/j.bbabo.2017.01.003
7. Dietrich A. Transient receptor potential (TRP) channels in health and disease. *Cells*. 2019;8(5):413. doi:10.3390/cells8050413
8. Nilius B, Owsianik G. The transient receptor potential family of ion channels. *Genome Biol*. 2011;12(3):218. doi:10.1186/gb-2011-12-3-218
9. Cao QF, Qian SB, Wang N, Zhang L, Wang WM, Shen HB. TRPM2 mediates histone deacetylase inhibition-induced apoptosis in bladder cancer cells. *Cancer Biother Radiopharm*. 2015;30(2):87–93. doi:10.1089/cbr.2014.1697
10. Noyer L, Grolez GP, Prevarskaya N, Gkika D, Lemonnier L. TRPM8 and prostate: a cold case? *Pflugers Arch Eur J Phys*. 2018;470(10):1419–1429. doi:10.1007/s00424-018-2169-1
11. Liu T, Liao Y, Tao H, et al. RNA interference-mediated depletion of TRPM8 enhances the efficacy of epirubicin chemotherapy in prostate cancer LNCaP and PC3 cells. *Oncol Lett*. 2018;15(4):4129–4136. doi:10.3892/ol.2018.7847
12. Peng M, Wang Z, Yang Z, et al. Overexpression of short TRPM8 variant  $\alpha$  promotes cell migration and invasion, and decreases starvation-induced apoptosis in prostate cancer LNCaP cells. *Oncol Lett*. 2015;10(3):1378–1384. doi:10.3892/ol.2015.3373
13. Grolez GP, Gordiendko DV, Clarisse M, et al. TRPM8-androgen receptor association within lipid rafts promotes prostate cancer cell migration. *Cell Death Dis*. 2019;10(9):652. doi:10.1038/s41419-019-1891-8
14. Bai VU, Murthy S, Chinnakannu K, et al. Androgen regulated TRPM8 expression: a potential mRNA marker for metastatic prostate cancer detection in body fluids. *Int J Oncol*. 2010;36(2):443–450.
15. Liu Z, Wu H, Wei Z, et al. TRPM8: a potential target for cancer treatment. *J Cancer Res Clin Oncol*. 2016;142(9):1871–1881. doi:10.1007/s00432-015-2112-1
16. Hantute-Ghesquier A, Haustrate A, Prevarskaya N, Lehen'kyi V. TRPM family channels in cancer. *Pharmaceuticals*. 2018;11(2):58. doi:10.3390/ph11020058
17. Yee NS, Zhou W, Lee M. Transient receptor potential channel TRPM8 is over-expressed and required for cellular proliferation in pancreatic adenocarcinoma. *Cancer Lett*. 2010;297(1):49–55. doi:10.1016/j.canlet.2010.04.023
18. Ceylan GG, Onalan EE, Kuloglu T, et al. Potential role of melastatin-related transient receptor potential cation channel subfamily M gene expression in the pathogenesis of urinary bladder cancer. *Oncol Lett*. 2016;12(6):5235–5239. doi:10.3892/ol.2016.5359
19. Xiao N, Jiang LM, Ge B, Zhang TY, Zhao XK, Zhou X. Over-expression of TRPM8 is associated with poor prognosis in urothelial carcinoma of bladder. *Tumour Biol*. 2014;35(11):11499–11504. doi:10.1007/s13277-014-2480-1

20. Li Q, Wang X, Yang Z, Wang B, Li S. Menthol induces cell death via the TRPM8 channel in the human bladder cancer cell line T24. *Oncology*. 2009;77(6):335–341. doi:10.1159/000264627
21. European Union. Directive 2010/63/EU of the European Parliament and of the Council of 22 September 2010 on the protection of animals used for scientific purposes. *OJEU*. 2010;L276:33.
22. Moloney JN, Cotter TG. ROS signalling in the biology of cancer. *Semin Cell Dev Biol*. 2018;80:50–64. doi:10.1016/j.semedb.2017.05.023
23. Park YS, You SY, Cho S, et al. Eccentric localization of catalase to protect chromosomes from oxidative damages during meiotic maturation in mouse oocytes. *Histochem Cell Biol*. 2016;146(3):281–288. doi:10.1007/s00418-016-1446-3
24. Wang Y, Zhao CS. Sigma-1 receptor activation ameliorates LPS-induced NO production and ROS formation through the Nrf2/HO-1 signaling pathway in cultured astrocytes. *Neurosci Lett*. 2019;711:134387. doi:10.1016/j.neulet.2019.134387
25. Cheng Y, Dai C, Zhang J. SIRT3-SOD2-ROS pathway is involved in linalool-induced glioma cell apoptotic death. *Acta biochimica Polonica*. 2017;64(2):343–350. doi:10.18388/abp.2016\_1438
26. Cao R, Wang G, Qian K, et al. TM4SF1 regulates apoptosis, cell cycle and ROS metabolism via the PPAR $\gamma$ -SIRT1 feedback loop in human bladder cancer cells. *Cancer Lett*. 2018;414:278–293. doi:10.1016/j.canlet.2017.11.015
27. Hu Q, Wang G, Peng J, et al. Knockdown of SIRT1 suppresses bladder cancer cell proliferation and migration and induces cell cycle arrest and antioxidant response through FOXO3a-mediated pathways. *Biomed Res Int*. 2017;2017:3781904. doi:10.1155/2017/3781904
28. Saitoh M. Involvement of partial EMT in cancer progression. *J Biochem*. 2018;164(4):257–264. doi:10.1093/jb/mvy047
29. Xu L, Zhang Y, Wang H, Zhang G, Ding Y, Zhao L. Tumor suppressor miR-1 restrains epithelial-mesenchymal transition and metastasis of colorectal carcinoma via the MAPK and PI3K/AKT pathway. *J Transl Med*. 2014;12:244. doi:10.1186/s12967-014-0244-8
30. Zhou Q, Chen J, Feng J, Xu Y, Zheng W, Wang J. SOSTDC1 inhibits follicular thyroid cancer cell proliferation, migration, and EMT via suppressing PI3K/Akt and MAPK/Erk signaling pathways. *Mol Cell Biochem*. 2017;435(1–2):87–95. doi:10.1007/s11010-017-3059-0
31. Mergler S, Mertens C, Valtink M, et al. Functional significance of thermosensitive transient receptor potential melastatin channel 8 (TRPM8) expression in immortalized human corneal endothelial cells. *Exp Eye Res*. 2013;116:337–349. doi:10.1016/j.exer.2013.10.003
32. Duchrow M, Schluter C, Key G, et al. Cell proliferation-associated nuclear antigen defined by antibody Ki-67: a new kind of cell cycle-maintaining proteins. *Arch Immunol Ther Exp*. 1995;43(2):117–121.

## OncoTargets and Therapy

### Publish your work in this journal

OncoTargets and Therapy is an international, peer-reviewed, open access journal focusing on the pathological basis of all cancers, potential targets for therapy and treatment protocols employed to improve the management of cancer patients. The journal also focuses on the impact of management programs and new therapeutic

agents and protocols on patient perspectives such as quality of life, adherence and satisfaction. The manuscript management system is completely online and includes a very quick and fair peer-review system, which is all easy to use. Visit <http://www.dovepress.com/testimonials.php> to read real quotes from published authors.

Submit your manuscript here: <https://www.dovepress.com/oncotargets-and-therapy-journal>

Dovepress